

Aristolochic acid nephropathy revisited: a place for innate and adaptive immunity?

Agnieszka A Pozdzik,^{1,2*} Alix Berton,³ Heinz H Schmeiser,⁴ Wassim Missoum,² Christine Decaestecker,^{5†} Isabelle J Salmon,³ Jean-Louis Vanherweghem² & Joëlle L Nortier^{1,2}
¹Unit of Experimental Nephrology, Faculty of Medicine, ²Nephrology and ³Pathology Departments, Erasme Hospital, Université Libre de Bruxelles, Brussels, Belgium, ⁴Division of Molecular Toxicology, German Cancer Research Institute, Heidelberg, Germany, and ⁵Laboratory of Toxicology, Institute of Pharmacy, Université Libre de Bruxelles, Brussels, Belgium

Date of submission 5 January 2009
Accepted for publication 30 June 2009

Pozdzik A A, Berton A, Schmeiser H H, Missoum W, Decaestecker C, Salmon I J, Vanherweghem J-L & Nortier J L (2010) *Histopathology* 56, 449–463

Aristolochic acid nephropathy revisited: a place for innate and adaptive immunity?

Aims: The histological features of aristolochic acid nephropathy (AAN) consist of paucicellular interstitial fibrosis, severe tubular atrophy, and almost intact glomeruli with media lesions of interlobular arteries. As an early phase of interstitial inflammation preceded peritubular fibrosis in the rat model of AAN, the aim was to investigate the presence of inflammatory cells in human AAN.

Methods and results: Reports of confirmed cases and case series of AAN were reviewed in terms of interstitial inflammation and found to have very conflicting results. This prompted us to search for and characterize inflammatory cells within the native kidneys provided from four end-stage AAN patients. Prior aristolochic acid exposure was attested by the intrarenal presence

of the typical aristolactam I-derived DNA adduct. Besides the tubulointerstitial lesions usually seen in the cortex, a massive infiltration of macrophages, T and B lymphocytes was detected by immunohistochemistry in the medullary rays and in the outer medullae with some extension to the upper cortical labyrinth.

Conclusions: In parallel with histological findings reported in the rat model, inflammatory cells are present preferentially in the interstitium of the medullary rays and of the outer medullae in renal interstitium from human AAN cases, even in the terminal stages. Further studies must be undertaken to determine the respective roles of innate and adaptive immunity in the progression of AAN.

Keywords: aristolochic acid, cytotoxic T cells, interstitial inflammation, macrophages, renal fibrosis

Abbreviations: α -SMA, alpha-smooth muscle actin; AA, aristolochic acid; AAI, aristolactam I; AAN, aristolochic acid nephropathy; ATP, adenosine triphosphate; CS, corticosteroid; ESRD, end-stage renal disease; FVIII, factor VIII/von Willebrand factor; IM, inner medullae; Mn/M ϕ , monocytes/macrophages; NEP, neutral endopeptidase; OM, outer medullae; PTEC, proximal tubular epithelial cell(s); TGF- β , transforming growth factor-beta; Th, T-helper

Introduction

Aristolochic acid nephropathy (AAN) is a rapidly progressive tubulointerstitial nephritis of toxic origin characterized by extensive renal fibrosis resulting in end-stage renal disease (ESRD).¹ The clinical syndrome

of so-called 'Chinese-herb nephropathy' was originally described in 1993 in Belgian women who had ingested root extracts of *Aristolochia fangchi* for slimming purposes over a mean time period of 15 months.^{1–3} Since that time, many cases have been reported around the world in relation to long-term traditional use of

Address for correspondence: J L Nortier, MD, PhD, Nephrology Department, Erasme Hospital, Université Libre de Bruxelles, Route de Lennik 808, B-1070 Brussels, Belgium. e-mail: joëlle.nortier@erasme.ulb.ac.be

*A.A.P. is a research fellow in Nephrology of the Université Libre de Bruxelles (Brussels, Belgium).

†C.D. is a senior research associate with the Belgian Research Found for Fundamental Research (FNRS, Belgium).

medicinal herbs containing *Aristolochia* species.⁴ The detection of DNA adducts formed by metabolites of aristolochic acid (AA) aristolactams in tissue samples of kidneys and ureters removed from AAN patients confirms prior exposure to AA.^{5–8} These specific adducts are known to induce carcinogenesis and mutagenesis by activation of H-ras proto-oncogene in rats and by p53 gene mutation in humans.⁹ p53 protein tissue overexpression¹⁰ is related to atypia, as well as the onset of multifocal transitional cell carcinoma in end-stage AAN patients.^{6,10–13}

Until now, the unique pathological picture of AAN has been of a diffuse, 'paucicellular' interstitial fibrosis with decreasing cortico-medullary gradient and marked tubular atrophy. Some vascular lesions (thickening of the intima and media of interlobar arteries) and urothelial atypia may also be present.^{12,14}

Actually, the pathophysiological mechanisms of the rapid progression of AAN to ESRD¹⁵ remain unclear. We investigated the time course of AA-induced tubulointerstitial lesions in a AAN rat model.¹⁶ Daily subcutaneous AA injections induced early and transient necrosis of proximal tubular epithelial cells (PTEC) (acute phase, days 4–5) followed by tubular atrophy and interstitial fibrosis (chronic phase, days 7–35).¹⁷ All tubulointerstitial lesions were limited to the external parts of medullary rays corresponding to the *pars recta* of proximal tubules (S3 segment).^{17,18} Interestingly, the acute phase was marked by interstitial foci of mononuclear cells around the necrotic tubules.¹⁹ Activated monocytes/macrophages (Mn/M ϕ) and cytotoxic CD8+ and CD4+ T lymphocytes clearly preceded fibrotic lesions but were still present during the chronic phase.^{17,19} These findings underline the involvement of immune cells in the progression of experimental AAN.

In the present study, we first sought a description of inflammatory cells in published cases of human AAN. We secondly took the opportunity to evaluate by immunohistochemistry the pattern and localization of interstitial inflammation in renal tissue samples from four AAN patients. Based on our pathological findings, we confirm the presence of an immune response to AA intoxication within the human kidney and propose a unifying physiopathological hypothesis of AAN progression involving innate and adaptive immunity.

Materials and methods

LITERATURE REVIEW

We reviewed all case reports or case series of AAN published in the literature written in English. The

articles were selected on the following criteria: (i) the pathological aspects were well described; (ii) previous exposure to AA was demonstrated either by the detection of AA-DNA adducts in the kidney and/or the presence of AA in the herbal preparation ingested by the patients.

PATIENTS AND KIDNEY TISSUE COLLECTION

According to an internal policy in our Nephrology Department, the surgical removal of native kidneys and ureters was proposed for all our end-stage AAN patients, considering the high risk of upper tract urothelial carcinoma.⁶ The present study focused on four unpublished cases: patients 1–3 (B..., S.; G..., A. and C..., F.) ingested slimming pills containing Chinese herbs (formula 2 regimen as described in the original publication¹ where the so-called *Stephania tetrandra* was inadvertently replaced by *A. fangji*); patient 4 (Y..., Q.) regularly ingested Chinese herbal tea bought in a Shanghai market over many years.

As positive controls of renal interstitial infiltration, we used tissue samples of kidney allograft provided from three patients (P..., M., L..., G. and D..., A.) suffering from chronic allograft rejection.

As negative controls, we used tissue samples available from three normal kidneys. All tissue samples were fixed in 4% paraformaldehyde and embedded in paraffin for morphological and immunohistochemical evaluations. In AAN patients, an additional sample of renal cortex was frozen and stored at -80°C for subsequent DNA isolation.

DETECTION OF AA-DNA ADDUCTS IN RENAL TISSUE SAMPLES FROM AAN PATIENTS

The DNA isolation from renal cortex tissue was performed by a standard phenol extraction method and analysed by the nuclease P1 enrichment version of the ³²P-postlabelling method.⁵ Briefly, DNA (12.5 μg) was digested with micrococcal nuclease (750 mU) and spleen phosphodiesterase (12.5 mU) in digestion buffer (20 mM sodium succinate, 8 mM CaCl₂, pH 6.0) for 3 h at 37°C in a total volume of 12.5 μl . Digests (2.5 μl) were removed and diluted 1:1500 to determine the amount of normal nucleotides. Digests (10 μl) were enriched for adducts by incubation with 5 μg (5 U) of nuclease P1 for 30 min at 37°C. Labelling mix (4 μl) consisting of 400 mM bicine (pH 9.5), 300 mM dithiothreitol, 200 mM MgCl₂, 10 mM spermidine, 100 μCi γ -³²P-adenosine triphosphate (ATP) (15 pmol), 0.5 μl 90 μM ATP and 10 U T4 polynucleotide kinase was added. After incubation for 30 min, 20 μl

was applied to a polyethylenimine-coated cellulose thin-layer chromatography plate (Macherey-Nagel, Düren, Germany) and chromatographed as described.⁵ Adducts and normal nucleotides were detected and quantified by an Instant Imager (Packard Inc., Canberra, Australia). Count rates of adducted fractions were determined from triplicate maps after subtraction of count rates from adjacent blank areas. Excess γ -³²P-ATP after the post-labelling reaction was confirmed. Adduct levels were calculated in units of relative adduct labelling, which is the ratio of cpm of adducted nucleotides to cpm of total nucleotides in the assay and were expressed as DNA adducts per 10⁸ normal nucleotides.

RENAL HISTOPATHOLOGY

Semiquantification of tubulointerstitial injury was performed on haematoxylin/eosin, periodic acid–Schiff, Goldner's trichrome and Red Sirius-stained sections as detailed previously.¹⁴ Total kidney samples were analysed with a light microscope (Carl Zeiss, Oberkochen, Germany) using a $\times 20$ magnification lens by three investigators (A.A.P., W.M. and I.J.S.). The scoring systems were defined as follows: tubular necrosis – 0, absent; 1, one group or a single necrotic tubule; 2, several clusters of necrotic tubules; 3, confluence of

necrotic clusters; tubular atrophy – 0, normal tubules; 1, one group or a single atrophic tubule; 2, several clusters of atrophic tubules; 3, confluence of atrophic tubular clusters; lymphocytic infiltrate – 0, absent; 1, few scattered cells; 2, group of lymphocytes; 3, dense widespread infiltrate; interstitial fibrosis – 0, absent; 1, mild diffuse fibrosis; 2, moderate fibrosis (less than one-third of the microscopic field); 3, severe fibrosis (more than one-third of the microscopic field). The scores given by the nephrologists and the pathologist were compared. If differences occurred, the sections were re-examined until a consensus was obtained. Urothelial tumours were graded and staged according to the 2004 World Health Organization Classification and the 2002 Union of International Cancer Classification-Tumour Node Metastasis Classification, respectively.¹³

IMMUNOHISTOCHEMISTRY

Tubular atrophy of proximal cells was attested by the expression of neutral endopeptidase (NEP) using monoclonal mouse anti-CD10 (LabVision, Fremont, CA, USA). Tubulointerstitial fibrosis was evaluated by immunostaining of collagen type I using monoclonal mouse anti-collagen I antibody (Abcam, Cambridge, UK). Mesenchymal cell and myofibroblast localization was determined by the use of monoclonal mouse

Table 1. Primary antibodies used for immunohistochemistry

| Antibodies | Clone | Laboratory | Dilution | Pre-treatment |
|------------|-------------------|------------------------------|------------|------------------------|
| CD4 | 1F6 | LabVision, Fremont, CA, USA | 1:50 | MW: EDTA 3 \times |
| CD8a | C8/144B | Novocastra, Newcastle, UK | 1:200 | MW: citrate 2 \times |
| CD20 | L26 | Dako, Heverlee, Belgium | 1:100 | MW: citrate 2 \times |
| CD45 | RP2/18 | Novocastra | 1:100 | – |
| CD68 | KP11 | Dako | 1:800 | MW: citrate 2 \times |
| CD34 | QBEND/10 | BioGenex, San Ramon, CA, USA | 1:30 | – |
| Collagen I | COLL-1 | Abcam, Cambridge, UK | 1:300 | MW: citrate 2 \times |
| FVIII | Rabbit polyclonal | Dako | 1:400 | Proteinase K:10 min |
| Granzyme | GZB01 | LabVision | Prediluted | MW: citrate 2 \times |
| Ki67 | MIB-1 | Dako | 1:1000 | MW: citrate 3 \times |
| NEP | 56C6 | LabVision | 1:300 | MW: citrate 2 \times |
| A-SMA | a-sm1 | Novocastra | 1:50 | – |
| Vimentin | V9 | Biogenex | 1:200 | – |

EDTA, Ethylenediamine tetraacetic acid.

Table 2. Review of histological data of published cases or series concerning aristolochic acid-related renal injury

| First author, year | Cases (<i>n</i>) | Interstitial inflammation | | | | | PL | Interstitial fibrosis |
|-----------------------------------------|-----------------------|---------------------------|----|----|-------------|-----|----------------------------------|-------------------------------------------------------|
| | | PMN | EO | MA | Mn/M ϕ | LYM | | |
| Acute renal injury Yang, 2007 | 8 | – | – | – | – | – | – | TGF- β in mononuclear cells |
| Fanconi syndrome Tanaka, 2000 | 2 | 0 | 0 | 0 | 0 | 0 | 0 | Paucicellular |
| Tanaka, 2000 | 4 | 0 | 0 | 0 | 0 | 0 | 0 | CM gradient |
| Tanaka, 2001 | 5 | 0 | 0 | 0 | 0 | 0 | 0 | CM gradient |
| Yang, 2002 | 1 | – | – | – | – | – | – | Acellular |
| Lee, 2004 | 1 | – | – | – | – | – | – | Severe |
| Hong, 2006 | 1 | – | – | – | – | – | – | Inflammatory cell infiltration |
| Chronic renal injury Reginster, 1997 | 2 | 0 | 0 | 0 | 0 | 0 | – | Diffuse |
| Vanherweghem, 1993 and 1994 | 8 | – | – | – | – | – | – | Extensive fibrosis |
| Jadoul, 1993 | 1 | – | – | – | – | – | – | Diffuse, CM gradient, mild inflammation |
| Schmeiser, 1996 | 5 | – | – | – | – | – | – | Extensive, hypocellular |
| Bieler, 1997 | 6 | – | – | – | – | – | – | Extensive, hypocellular |
| Cosyns, 1999 | 10 | – | – | – | – | – | – | – |
| Ubara, 1999 | 1 | – | – | – | – | – | – | Marked with mild inflammation |
| Gillerot, 2001 | 1 | – | – | – | – | – | – | Extensive hypocellular |
| Cronin, 2002 | 2 | – | – | – | – | – | – | Cortical |
| Nortier, 2003 | 1 | – | – | – | – | – | – | Interstitial |
| Kanaan, 2003 | 2 | – | – | – | – | – | – | Acellular, infiltration of medullary rays |
| Hoshino, 2003 | 1 | – | – | – | – | – | – | Extensive tubulointerstitial, scant cell infiltration |
| Lo, 2005 | 1 | – | – | – | – | – | – | Hypocellular |
| Depierreux, 1994 | 33 | Nearly absent | – | – | – | – | Clusters around atrophic tubules | Paucicellular, CM gradient |
| Cosyns, 1994 | 3 | Rare | – | – | – | – | Scattered, in the cortex | Diffuse, paucicellular, CM gradient |

Table 2. (Continued)

| First author, year | Cases (n) | Interstitial inflammation | | | | | PL | Interstitial fibrosis |
|--------------------|-----------|---------------------------|----|----|-------------|---------------------------------------------|----|----------------------------|
| | | PMN | EO | MA | Mn/M ϕ | LYM | | |
| Vanherweghem, 1995 | 1 | - | - | - | - | Scattered, around atrophic tubules | - | - |
| Lord, 1999 | 1 | - | - | - | - | Mononuclear cell infiltration in the cortex | - | Paucicellular, CM gradient |
| Meyer, 2000 | 1 | 0 | - | - | - | Focal lymphocyte infiltration | - | Extensive |
| Nishimagi, 2001 | 1 | - | - | - | - | Focal lymphocyte infiltration | - | Severe |
| Lo, 2004 | 1 | + | + | - | - | In the interstitium | + | Significant |
| Yang, 2006 | 1 | - | - | - | - | Moderate inflammatory cell infiltration | - | Diffuse |

n, number; PMN, polymorphonuclear cell; EO, eosinophil; MA, mast cells; Mn/M ϕ , monocyte/macrophage; LYM, lymphocyte; PL, plasmacyte; -, unavailable; +, presence; 0, absence; CM, corticomedullary.

anti-vimentin (Biogenex, San Ramon, CA, USA) and antialpha-smooth muscle actin (α -SMA) (Novocastra, Newcastle, UK) antibodies, respectively. Vessels were identified by factor VIII/von Willebrand factor (FVIII) and CD34 endothelial expression (polyclonal rabbit anti-FVIII from Dako, Heverlee, Belgium and monoclonal mouse anti-CD34 from BioGenex, respectively). Infiltrating Mn/M ϕ , total leucocytes, B lymphocytes, T-helper (Th) lymphocytes, T cytotoxic/suppressor lymphocytes and natural killer cells were identified using the respective following monoclonal mouse primary antibodies: anti-CD68 (Dako), antiCD45 (Novocastra), antiCD20 (Dako), antiCD4 (LabVision) and antiCD8a (Novocastra). The cytotoxic T lymphocyte granzyme B was assessed by mouse monoclonal antigranzyme B (LabVision). Cell proliferation was evaluated by Ki67 expression (mouse monoclonal antiKi67 from Dako).

Immunohistochemistry with all primary antibodies was performed on longitudinal paraffin-embedded sections (5 μ m) attached to poly-L-lysine pretreated slides (Sigma-Aldrich, Bornem, Belgium) (Table 1). Avidin-biotin complex enzyme revealing technology immunohistochemistry was performed as previously described (specific conditions for immunohistochemistry are detailed in Table 1).^{17,20} Diaminobenzidine/hydrogen peroxide was used as the chromogene substrate producing a brown end-product. All reagents were provided from Vector Laboratories (Burlingame, CA, USA). Counterstaining with haematoxylin completed

the processing. After dehydration through alcohols and toluene, the slides were immediately mounted in permanent, organic mounting medium (DPX; VWR International, Leuven, Belgium) and covered with a glass coverslip.

The specificity and the pattern of each antibody were tested on positive control tissue samples according to the manufacturers' technical data.

We used negative controls of two types for each labelling. A normal horse serum (5% solution) instead of primary antibody (used in order to exclude non-specific kit reagent staining) and mouse IgG, mouse IgM or rabbit IgG immunoglobulin isotypes (used in order to exclude non-specific staining of immunoglobulin binding sites). None showed any positive staining.

SEMIQUANTITATIVE EVALUATIONS

Evaluation of all immunochemistry was performed by two investigators (A.A.P. and W.M.).

Semiquantification of NEP and of vimentin, α -SMA and type I collagen immunoreactivity reflecting tubular atrophy and interstitial fibrosis, respectively, were performed as follows: 0, absence of fibrosis; 1, scattered fibrotic areas (less than one-third of the microscopic field); 2, moderate fibrosis (less than two-thirds of the microscopic field); 3, extensive fibrosis (more than two-thirds of the microscopic field). Total kidney samples were analysed with a light microscope (Carl Zeiss) using a $\times 20$ magnification lens.

Positively stained interstitial mononuclear cells were counted with a $\times 40$ magnification lens in 50 fields corresponding to $2.88 \mu\text{m}^2$ (50×0.058) of tissue area. Results were expressed as the average number of positively stained cells per field.

Results

LITERATURE REVIEW

Almost all published histological findings are related to pre-terminal or end-stage AAN (summarized in Table 2). Nephrotoxicity of AA in Japan seems to be limited to a Fanconi syndrome without any malignancy of the urinary tract.^{21–26} Only one study demonstrated acute AA tubulotoxicity.^{24,27} The absence of inflammatory cells has been reported in a few publications.^{15,21–23} In the majority of pathological reports, interstitial inflammation has not been assessed.^{1–3,5,7,10,24–26,28–36} In some reports

taking into account interstitial inflammation,^{12,14,37–41} characterization of the infiltrating cells was not available.

CLINICAL CHARACTERISTICS

None of our AAN patients considered in the present study was a regular user of analgesics or anti-inflammatory non-steroidal drugs. Except for patient B...S., who had a left reflux, none had a personal or family history of renal disease, cardiovascular disease, systemic hypertension, diabetes mellitus or hypercholesterolaemia (Table 3). All patients with chronic allograft rejection were treated for hypercholesterolaemia and hypertension.

AA-DNA ADDUCTS

The specific AA-DNA adduct, 7-(deoxyadenosin-N6-yl)-aristolactam I (dA-AAI), was identified in renal

Table 3. Clinical data from studied patients

| Characteristics/variables | B..., S. | G..., A. | C..., F. | Y..., Q. | P..., M. | L..., G. | D..., A. |
|--------------------------------------------------------|----------------|---------------|-----------------|-----------------|-------------|-------------|-------------|
| Age (years) | 50 | 65 | 59 | 51 | 57 | 42 | 45 |
| Risk factors for renal disease | | | | | | | |
| Familial | No | No | No | No | No | No | No |
| Personal | Reflux left | No | No | No | No | No | No |
| Diabetes mellitus | No | No | No | No | No | No | No |
| Hypertension | No | No | No | No | Yes | Yes | Yes |
| Hypercholesterolaemia | No | No | No | No | Yes | Yes | Yes |
| Mesotherapy | Yes | Yes | Yes | No | No | No | No |
| Analgesics intake | No | No | No | No | No | No | No |
| NSAID intake | No | No | No | No | No | No | No |
| Period of exposition for AA (months) | 2 | 12 | 8 | >120 | No exposure | No exposure | No exposure |
| Current treatment | KTx | KTx | HD | CAPD | HD | KTx | HD |
| Total ingested dose of <i>Aristolochia fangchi</i> (g) | 120 | 84 | 66 | Unknown | 0 | 0 | 0 |
| dA-AAI DNA adducts (per 10^8 normal nucleotides) | 3.5 ± 1.45 | 1.9 ± 0.9 | 6.25 ± 0.57 | 44.3 ± 11.1 | ND | ND | ND |

AAN, Aristolochic acid nephropathy; Cr, creatinine; GFR, glomerular filtration rate estimated by Cockcroft–Gault formula; KTx, kidney transplantation; HD, haemodialysis; CAPD, continuous ambulatory peritoneal dialysis; dA-AAI, 7-(deoxyadenosine-N⁶-yl) aristolactam I; NSAID, non-steroidal anti-inflammatory drugs.

tissue samples from our AAN patients, indicating permanent lesions within the genomic DNA (Table 3).

PATHOLOGICAL FINDINGS FROM REMOVED KIDNEYS

Macroscopically, the native kidneys from AAN cases were shrunken with a significantly reduced size of the cortex. The pelvis and ureters were unremarkable. No papillary necrosis, hydronephrosis or periureteral fibrosis were detected.

Microscopically, all kidney tissue samples disclosed the same type of alterations. Upon light microscopy, the capsula was thickened. An intense interstitial fibrosis

containing completely solidified glomeruli were predominantly seen in the cortex with a corticomedullary gradient (Figure 1A–D). Relatively spared glomeruli showing signs of ischaemia were found in the renal cortical labyrinth. Thickening of Bowman’s capsula was the rule.

Severe interstitial fibrosis and massive tubular atrophy resulted in the disappearance of tubules between the glomeruli, particularly in the cortex. All segments of tubules were affected. Atrophic tubules were still visible in the zones corresponding to the medullary rays and to the outer medullae (Figure 1A–D).

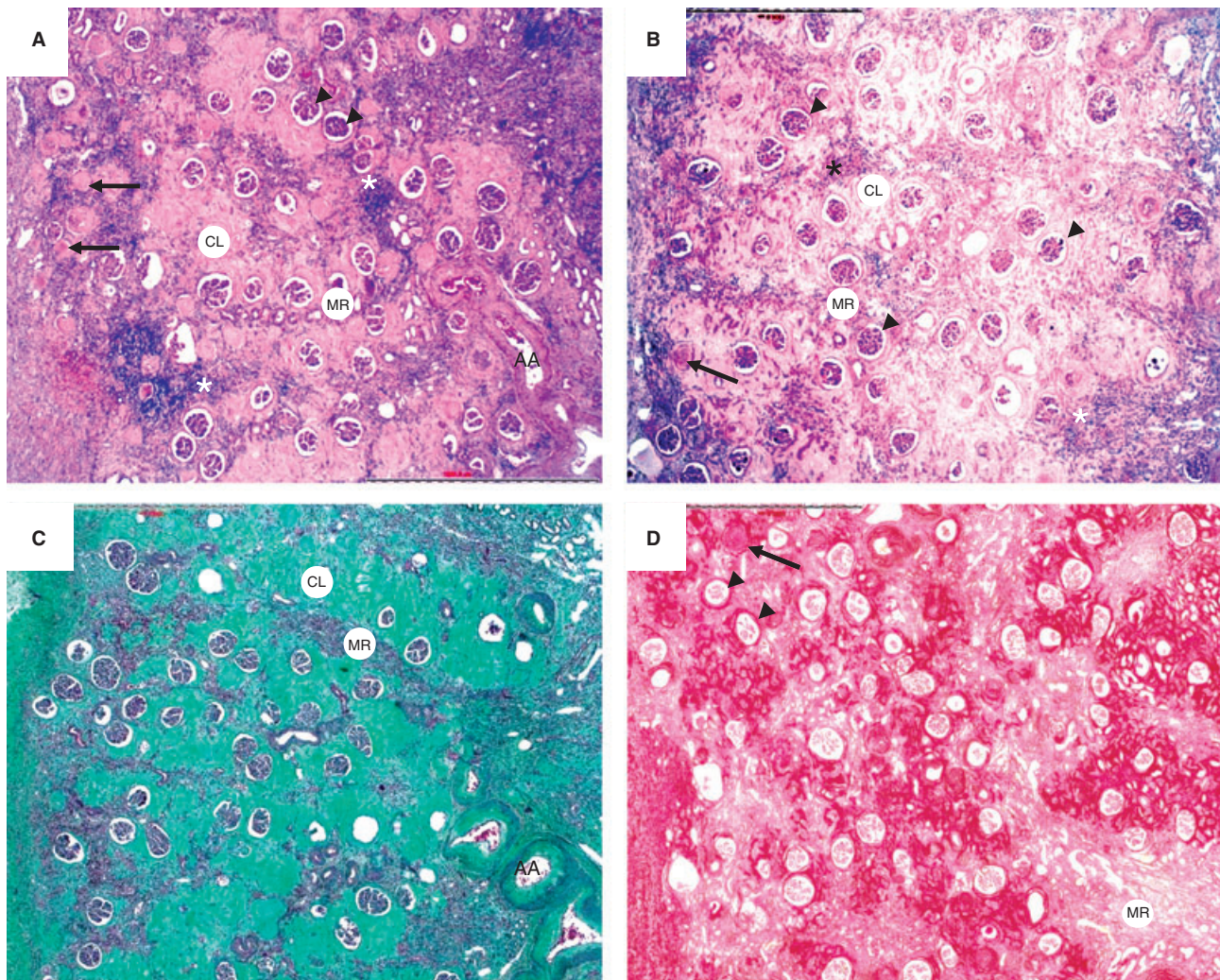


Figure 1. Photomicrographs showing representative lesions of the renal parenchyma from end-stage aristolochic acid nephropathy patients. Diffuse cortical atrophy with significant reduction of medullary rays (MR). Paucicellular interstitial fibrosis extending from the superficial cortex to the medullae. Solidified (arrows) and ischaemic glomeruli (arrowheads). Atrophic tubules present in the medullae. Foci of interstitial infiltrate around tubules in the pyramids and inner medullae (stars). Severe fibrous intimal thickening of arcuate artery (AA) A, H&E. B, Periodic acid–Schiff. C, Goldner’s Trichrome staining. D, Picro Sirius staining.

Table 4. Histopathological evaluations of tubulointerstitial injury and infiltrating cells

| Variables | Negative controls | | | AAN | | | | Positive controls | | |
|------------------------------------------------------------------------------------------------------------------------------------------------|-------------------|------|------|----------|----------|----------|----------|-------------------|---------|----------|
| | C1 | C2 | C3 | B..., S. | G..., A. | C..., F. | Y..., Q. | P..., M. | L..., G | D..., A. |
| Semiquantitative score of tubulointerstitial injury (0–3) | | | | | | | | | | |
| Tubular necrosis | 0 | 1 | 0 | 0 | 0 | 0 | 0 | 0 | 0 | 0 |
| Lymphocytic infiltration | 0 | 0 | 0 | 3 | 3 | 3 | 3 | 3 | 3 | 3 |
| Tubular atrophy | 0 | 0 | 0 | 3 | 3 | 3 | 3 | 3 | 2 | 3 |
| Interstitial fibrosis | 0 | 1 | 0 | 3 | 3 | 3 | 3 | 3 | 2 | 3 |
| Semiquantitative scores of tubular atrophy (0–3) evaluated by NEP expression | | | | | | | | | | |
| NEP | 3 | 2 | 3 | 1 | 1 | 1 | 1 | 2 | 1 | 0 |
| Semiquantitative scores of mesenchymal cells, myofibroblasts and collagen immunoreactivity (0–3) evaluated by expression of following antigens | | | | | | | | | | |
| Vimentin | 0 | 0 | 0 | 3 | 3 | 3 | 3 | 3 | 3 | 2 |
| α -SMA | 1 | 1 | 1 | 3 | 3 | 3 | 3 | 3 | 2 | 2 |
| Collagen type I | ND | ND | ND | 3 | 3 | 3 | 3 | 3 | 2 | 2 |
| Quantification of interstitial mononuclear cell infiltrates and proliferation assessment (average number of immunopositive cells/field) | | | | | | | | | | |
| CD68 | 0.88 | 0.86 | 0.44 | 6.10 | 27.8 | 13.9 | 4.16 | 35.1 | 33.6 | 40.8 |
| CD45 | 0.04 | 0.40 | 0.76 | 24.3 | 27.6 | 39.2 | 92.5 | 134 | 129 | 135 |
| CD20 | 0.00 | 0.02 | 0.00 | 18.6 | 33.7 | 16.6 | 137 | 18.7 | 27.9 | 39.2 |
| CD4 | 0.00 | 0.06 | 0.30 | 44.7 | 38.5 | 49.3 | 138 | 63.9 | 66.0 | 76.1 |
| CD8a | 0.24 | 0.46 | 0.90 | 77.3 | 84.9 | 41.6 | 69.9 | 54.1 | 63.4 | 56.2 |
| Ki67 | 0.04 | 0.02 | 0.00 | 1.92 | 0.46 | 1.92 | 0.08 | 2.92 | 0.12 | 30.2 |

AAN, Aristolochic acid nephropathy; NEP, neutral endopeptidase; α -SMA, alpha-smooth muscle actin.

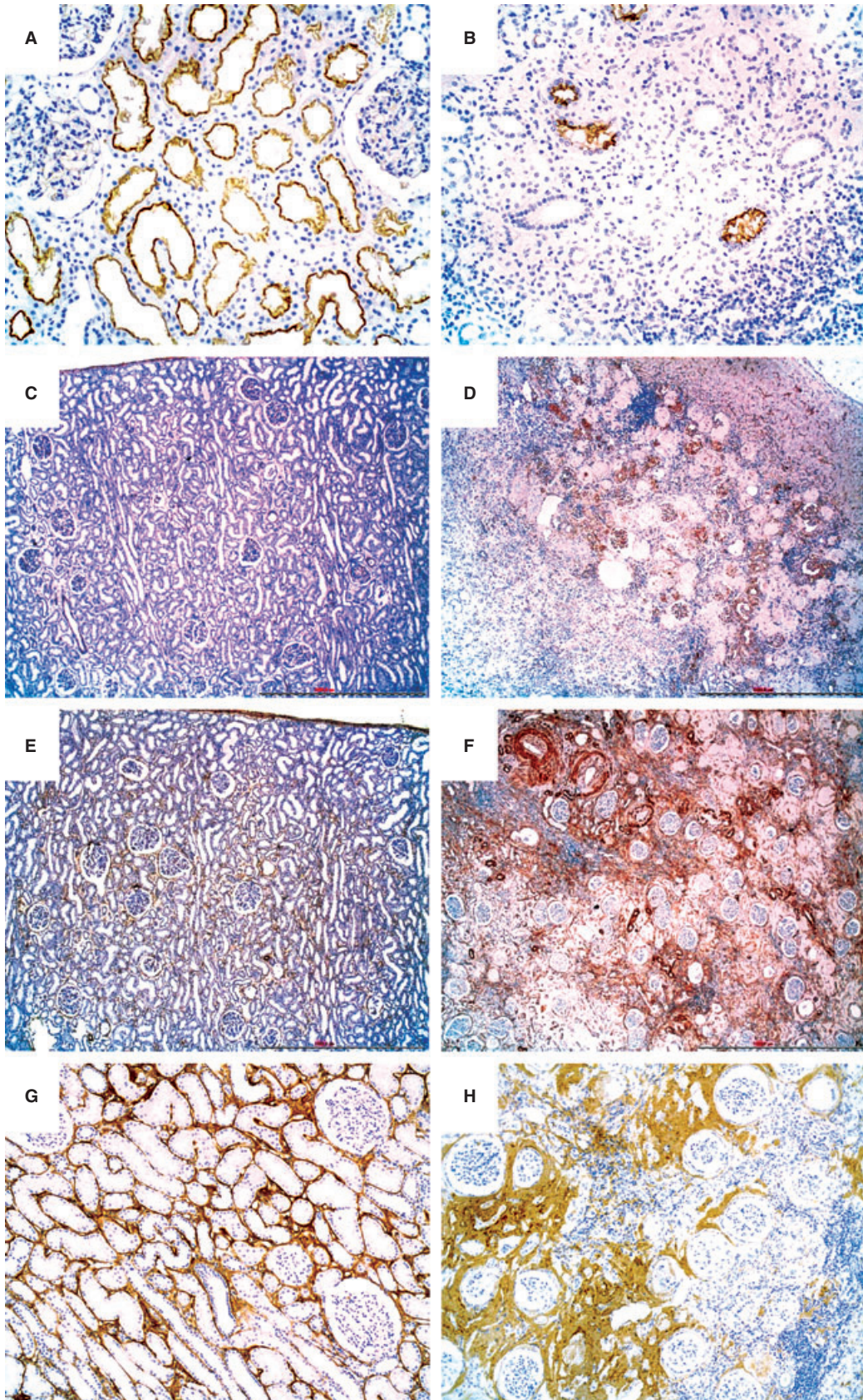
All vessels exhibited major lesions of the intima and media. Marked thickening of the walls resulted in lumen reduction in the arcuate and interlobular arteries (Figure 1B,C).

In the medullary rays and in the outer medullae (MR and OM), atrophic tubules were surrounded by clusters of interstitial mononuclear cells (Figure 1A). No neutrophilic or eosinophilic polymorphonuclear cells

as well as mast cells were found. No necrosis of tubular epithelial cells was present.

Extensive fibrosis, marked tubular atrophy and interstitial inflammation were evident, as assessed by the semiquantitative score of tubulointerstitial injury (Table 4). Mild to moderate urothelial dysplasia of the upper part of the right ureter was observed in Patient B..., S. In Patient Y..., G, carcinoma *in*

Figure 2. Renal expression of neutral endopeptidase (NEP), vimentin, alpha-smooth muscle actin (α -SMA) and type I collagen in controls and in aristolochic acid nephropathy (AAN) patients. In control kidney, the expression of NEP is limited to the brush border of proximal tubular epithelial cells (PTECs) and to the epithelium of Bowman's capsule (A). Marked loss of NEP from PTEC after aristolochic acid exposure (B). Vimentin expression by the Bowman's capsule and endothelial cells in a control kidney (C) contrasting with the enhanced vimentin expression by renal interstitial cells from an end-stage AAN patient (D). α -SMA expression by vessel walls in a control kidney (E) and dramatically enhanced α -SMA immunoreactivity in renal interstitial cells and vessels from an end-stage AAN patient (F). Compared with a control kidney (G), extensive collagen type I accumulation in the renal cortex from a representative AAN patient (H).



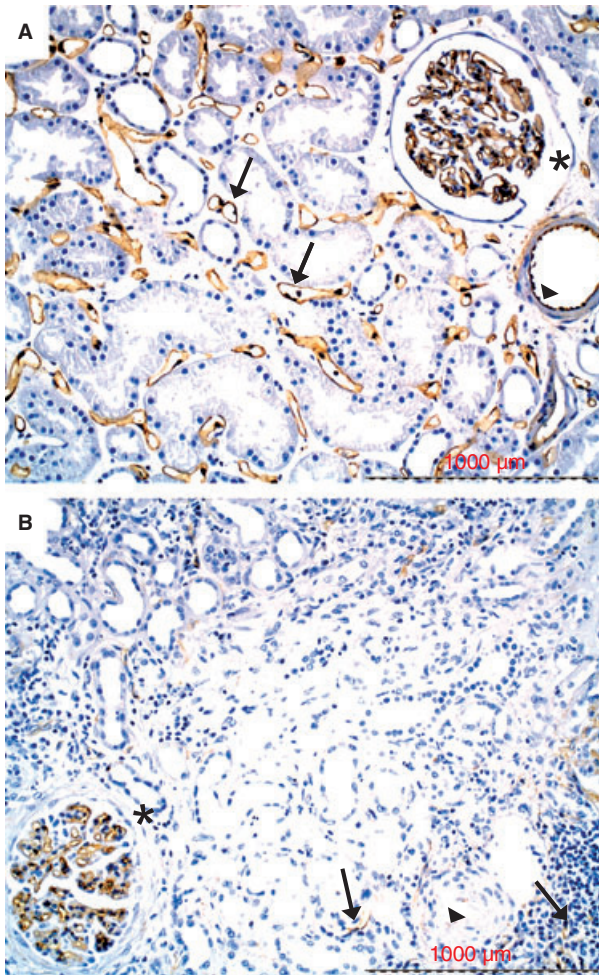


Figure 3. Renal expression of CD34 in control and aristolochic acid nephropathy (AAN) patients. Dense peritubular capillary network (arrows) as attested by endothelial expression of CD34 (arrowhead) in a control (A). Immunopositive CD34 glomeruli (stars) are found in control and AAN patients (B). Disappearance of peritubular capillaries in areas of interstitial scar (arrows) and marked rarefaction in the deeper part corresponding to areas of atrophic tubules in AAN patients.

situ was detected along the upper part of the right ureter.

TUBULAR ATROPHY AND INTERSTITIAL SCARRING

The NEP immunostaining reflecting the integrity of the PTEC brush border was almost absent, confirming severe atrophy (Figure 2A,B). Extensive vimentin expression

reflected the interstitial accumulation of mesenchymal cells: fibroblasts and probably lympho,haematopoietic cells (Figure 2C,D). Strong α -SMA expression confirmed the accumulation of interstitial myofibroblasts in the cortex (Figure 2E,F) associated with extensive type I collagen immunoreactivity (Figure 2G,H).

DISAPPEARANCE OF PERITUBULAR CAPILLARIES

In the fibrotic zones, the absence of peritubular capillaries was attested by endothelial CD34 immunoreactivity (Figure 3A,B). In the deeper cortex from AAN cases, the peritubular capillary network was still present but only in a few zones of atrophic tubules (Figure 3A,B).

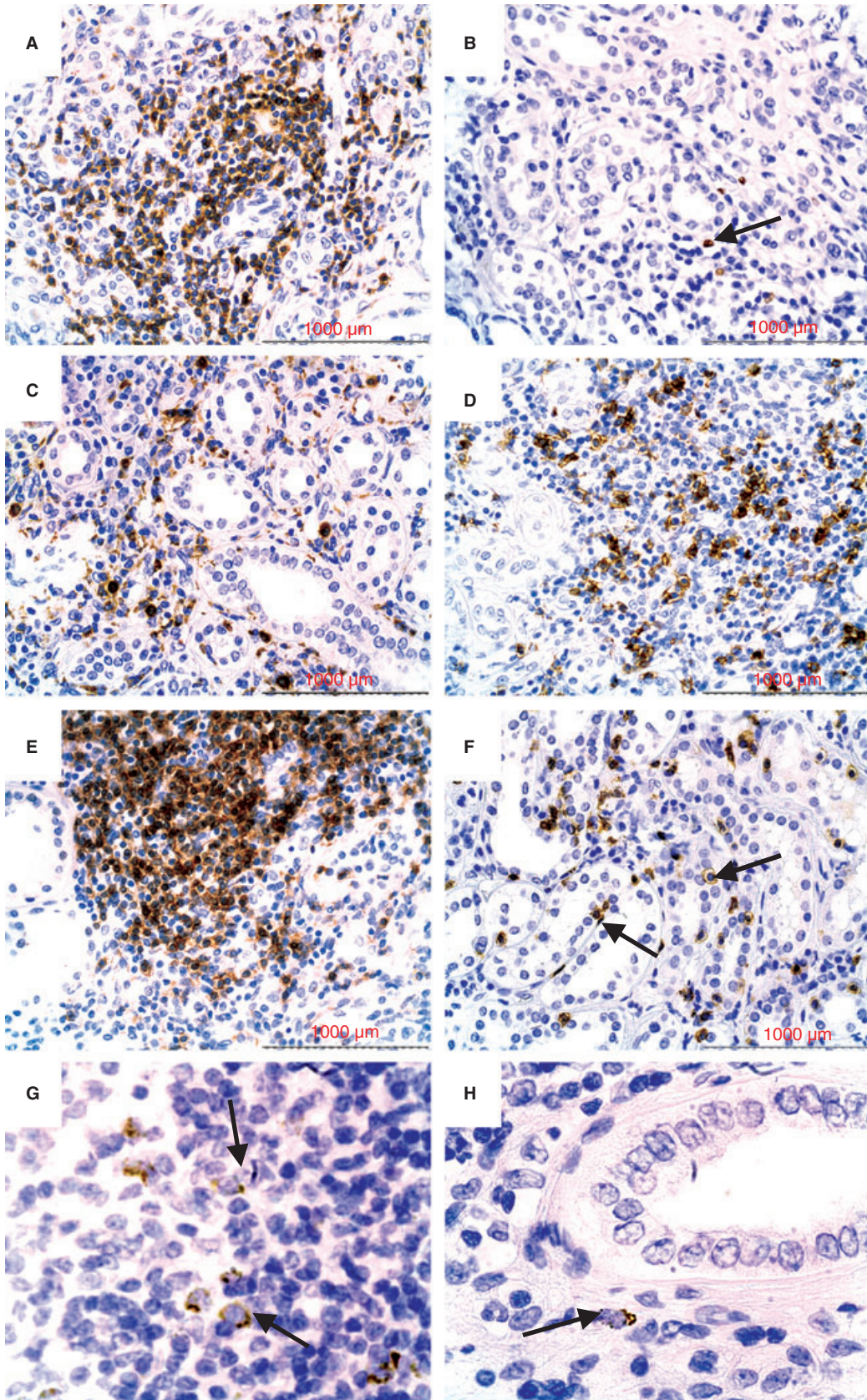
PHENOTYPE OF MONONUCLEAR INFLAMMATORY CELLS

As compared to positive controls, the renal parenchyma from AAN patients exhibited intense infiltration of MR and to some extent of the OM by leucocytes (CD45+-expressing cells) around degenerated tubules, contrasting with the absence of any infiltrate in the cortical labyrinth (Figure 4A, Table 4). Only rare interstitial cells expressed Ki67, whereas no proliferative activity was detected in tubular cells (Figure 4B, Table 4). Clusters of Mn/M ϕ (interstitial cells expressing CD68 antigen) were found around degenerated tubules in the MR and in the OM (Figure 4C, Table 3). The interstitial accumulation in the MR and in the OM with some extension to the superficial cortical labyrinth of B lymphocytes and CD4+ and CD8+ subsets of T lymphocytes (Figure 4D–F) was evident, as shown by semiquantitative evaluation of CD20, CD4 and CD8 immunostainings (Table 4). The cytotoxicity of infiltrating T lymphocytes was attested by the intraepithelial presence of CD8+ cells (tubulitis shown in Figure 4F), as well as the expression of granzyme B by some interstitial mononuclear cells (Figure 4G,H).

Discussion

A striking clinical characteristic of AAN is the rapid progression to ESRD despite discontinuation of the AA-containing herbal medication.¹ This implies that additional mechanisms are working in addition to

Figure 4. Immunohistochemistry of infiltrating mononuclear cells, Ki67 and granzyme B in renal tissue samples from aristolochic acid nephropathy (AAN) patients. Clusters of CD45+ cells (A). A few interstitial cells exhibit Ki67 expression (arrow) (B). CD68+, CD20+ and CD4+ cells forming interstitial clusters around atrophic tubules (C, D and E, respectively). Intraepithelial CD8+ cells (tubulitis; arrows) (F). Immunopositivity for granzyme B in mononuclear cells (arrows) (G). Positive control (human tonsil) and infiltrating renal interstitial cells from an end-stage AAN patient (arrow) (H).



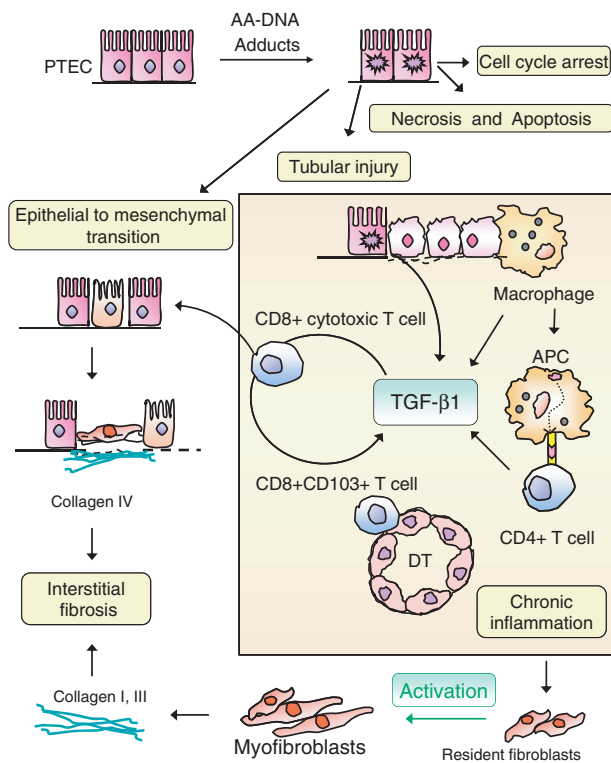


Figure 5. Physiopathological hypothesis of inflammatory cell involvement in the progression of aristolochic acid (AA)-induced renal interstitial fibrosis. Secondary to AA intoxication, the proximal tubular epithelial cells (PTEC) undergo necrosis and apoptosis as well as cell cycle arrest. The epithelial to mesenchymal transition is limited to PTEC, especially from the S3 segment. These dedifferentiated cells are the source of collagen IV. Necrotic cells and apoptotic bodies then stimulate macrophages; these cells dedifferentiate into antigen-presenting cells able to prime T cells. Damaged PTEC and interstitial inflammatory cells both secrete transforming growth factor-beta, which in turn activates resident fibroblasts into myofibroblasts producing collagen I and III.

AA direct tubulotoxicity, resulting in fibrogenesis. According to our observation, the bridge between these processes is the onset of an immune response. In this respect, conflicting results are available in the literature concerning the presence of inflammatory cells in kidney tissue samples obtained from biopsy or nephroureterectomy in pre-terminal or end-stage AAN patients (for summary see Table 2). There is a disparity in the description of the severity of the inflammatory process as well as its localization. Most available pathological data were obtained from the analysis of a small-sized renal cortical biopsy specimen. This limited material could explain the discrepancy in the observations reported by different authors.

The initial histological description of AAN lesions in patients from the Belgian cohort had already mentioned the presence of a lymphocytic infiltration.¹⁴ It

should be noted that, at the time of renal biopsy, serum creatinine levels ranged from 1.4 to 12.7 mg/dl. At the early stages of the renal disease, only sparse interstitial inflammatory cells were found. This was observed by others in human cases.³⁶ In the AAN rat model, early inflammation was also limited to the vicinity of necrotic tubules.^{17,19} Three weeks later, these areas were filled by collagen deposits concomitantly with severe tubular atrophy.^{17,19}

The possibility of another condition causing inflammation in the present cases has been excluded (Table 2). Classical risks factors for renal diseases were obtained from detailed retrospective analysis of the medical records of the patients according to the same methodology previously followed.⁴² Herbal remedies were prescribed only for weight loss. Three of these four patients were actually cared for by the same Belgian clinic specialized in slimming regimens as the first cases published from 1993 to 2000.^{6,42}

Data reported here have demonstrated the persistence of interstitial inflammatory cells even in end-stage AAN kidneys, as confirmed by the specific AA-DNA adducts in these tissue samples more than 10 years after cessation of AA exposure. For the first time to our knowledge, immunohistochemical evidence has led to the identification of Mn/M ϕ (innate immunity) and T lymphocytes (adaptive immunity). Progression of AAN could be related to the presence of cytotoxic CD8+ T lymphocytes, as attested by marked tubulitis and granzyme B expression and significant macrophage infiltration. Such kidney infiltration by CD8+ T lymphocytes has been shown to be involved in the progression of other toxic nephropathies.^{43–53} In our cohort, a pilot study with corticosteroid (CS) treatment resulted in a significant decrease in the progression rate of renal failure.⁵⁴ Other subsequent case reports in AAN patients with mild renal failure have confirmed the beneficial effect of CS administration in slowing down the progression of the disease.^{35,39,55,56} Anti-inflammatory CS properties could be related to the preferential enhancement of Th2 lymphocyte activity, leading to the neutralization of proinflammatory cytokines secreted by Th1 cells and activated macrophages.⁵⁷

On the other hand, our data limited to end-stage kidneys demonstrate a dramatic decrease in peritubular capillaries especially in the fibrotic areas. Some endothelial cells of remaining capillaries adjacent to atrophic tubules and from thickened arteries exhibited only weak CD34 immunoreactivity. However, suspected endothelial dysfunction could not be fully investigated. One study from Yang *et al.*³⁶ reported similar results of rarefaction of peritubular capillaries. Actually, changes

in the vascular compartment in AAN remain a challenge for the pathologist.

Finally, we propose the following mechanisms for AA-related interstitial fibrosis, as schematically represented in Figure 5. *In vitro* and *in vivo* studies have shown that PTEC are the preferential target of AA toxicity.^{17,18,58–60} Marked tubular atrophy could be, in part, secondary to AAI-induced cell cycle arrest secondary to DNA damage (replication phase), as recently reported by Simoes *et al.*⁶¹ The balance between apoptosis and necrosis of PTEC appears crucial in inducing immune cell interstitial infiltration. Phagocytosis of necrotic PTEC results in the activation of interstitial Mn/M ϕ into antigen-presenting cells able to prime a T-lymphocyte response.^{62,63} The innate and adaptive immunity cell components are proposed as the missing link between acute AA tubulotoxicity and subsequent interstitial fibrosis. Proinflammatory and pro-fibrosing cytokines are likely to be involved in these processes,^{64–66} at least monocyte chemoattractant protein-1 and transforming growth factor-beta (TGF- β).^{67–71} In our model of AAN, PTEC and interstitial cells both expressed TGF- β ,^{17,19} confirming Yang's data on human cases of the acute phase of AAN.³⁶ This persistent inflammation leads to resident fibroblast activation.^{68,72–76}

To summarize, the present data support the concept that innate and adaptive immunity is involved in the deleterious evolution of primarily non-immune kidney disease. Histological criteria of AAN diagnosis might be revisited taking into consideration the presence of interstitial inflammation. In addition, strategies able to modulate innate and adaptive immunity would be of great potential therapeutic benefit.

Acknowledgements

This study was supported by grants from the Belgian Research Fund for Fundamental Research (FNRS, Belgium). We are indebted to Drs D. Abramowicz, R. Bollens, N. Broeders, B. Guillaume, A. Hoang, D. Michalsky, C. Tielemans, T. Quackels and K. M. Wissing for care of the patients and to Dr M. Depierreux from pathology departments for helpful comments. We also thank the nursing and technical staffs of the Nephrology, Dialysis, and Renal Transplantation Departments for their continuous cooperation.

Competing interests

None to declare.

References

1. Vanherweghem JL, Depierreux M, Tielemans C *et al.* Rapidly progressive interstitial renal fibrosis in young women: association with slimming regimen including Chinese herbs. *Lancet* 1993; **341**: 387–391.
2. Jadoul M, De Plaen JF, Cosyns JP, Van Ypersele de Strihou C. Adverse effects from traditional Chinese medicine. *Lancet* 1993; **341**: 892–893.
3. Vanhaelen M, Vanhaelen-Fastre R, But P, Vanherweghem JL. Identification of aristolochic acid in Chinese herbs. *Lancet* 1994; **343**: 174.
4. Debelle FD, Vanherweghem JL, Nortier JL. Aristolochic acid nephropathy: a worldwide problem. *Kidney Int.* 2008; **74**: 158–169.
5. Schmeiser HH, Bieler CA, Wiessler M, Van Ypersele de Strihou C, Cosyns JP. Detection of DNA adducts formed by aristolochic acid in renal tissue from patients with Chinese herbs nephropathy. *Cancer Res.* 1996; **56**: 2025–2028.
6. Nortier JL, Martinez MC, Schmeiser HH *et al.* Urothelial carcinoma associated with the use of a Chinese herb (*Aristolochia fangchi*). *N. Engl. J. Med.* 2000; **342**: 1686–1692.
7. Bieler CA, Stiborova M, Wiessler M, Cosyns JP, Van Ypersele de Strihou C, Schmeiser HH. 32P-post-labelling analysis of DNA adducts formed by aristolochic acid in tissues from patients with Chinese herbs nephropathy. *Carcinogenesis* 1997; **18**: 1063–1067.
8. Stiborova M, Frei E, Breuer A, Bieler CA, Schmeiser HH. Aristolactam I a metabolite of aristolochic acid I upon activation forms an adduct found in DNA of patients with Chinese herbs nephropathy. *Exp. Toxicol. Pathol.* 1999; **51**: 421–427.
9. Schmeiser HH, Stiborova M, Arlt VM. Chemical and molecular basis of the carcinogenicity of Aristolochia plants. *Curr. Opin. Drug Discov. Devel.* 2009; **12**: 141–148.
10. Cosyns JP, Jadoul M, Squifflet JP, Wese FX, Van Ypersele de Strihou C. Urothelial lesions in Chinese-herb nephropathy. *Am. J. Kidney Dis.* 1999; **33**: 1011–1017.
11. Cosyns JP, Jadoul M, Squifflet JP, Van Cangh PJ, Van Ypersele de Strihou C. Urothelial malignancy in nephropathy due to Chinese herbs. *Lancet* 1994; **344**: 188.
12. Cosyns JP, Jadoul M, Squifflet JP, De Plaen JF, Ferluga D, Van Ypersele de Strihou C. Chinese herbs nephropathy: a clue to Balkan endemic nephropathy? *Kidney Int.* 1994; **45**: 1680–1688.
13. Lemy A, Wissing KM, Rorive S *et al.* Late onset of bladder urothelial carcinoma after kidney transplantation for end-stage aristolochic acid nephropathy: a case series with 15-year follow-up. *Am. J. Kidney Dis.* 2008; **51**: 471–477.
14. Depierreux M, Van Damme B, Vanden Houste K, Vanherweghem JL. Pathologic aspects of a newly described nephropathy related to the prolonged use of Chinese herbs. *Am. J. Kidney Dis.* 1994; **24**: 172–180.
15. Reginster F, Jadoul M, Van Ypersele de Strihou C. Chinese herbs nephropathy presentation, natural history and fate after transplantation. *Nephrol. Dial. Transplant.* 1997; **12**: 81–86.
16. Debelle FD, Nortier JL, De Prez EG *et al.* Aristolochic acids induce chronic renal failure with interstitial fibrosis in salt-depleted rats. *J. Am. Soc. Nephrol.* 2002; **13**: 431–436.
17. Pozdzik AA, Salmon IJ, Debelle FD *et al.* Aristolochic acid induces proximal tubule apoptosis and epithelial to mesenchymal transformation. *Kidney Int.* 2008; **73**: 595–607.
18. Lebeau C, Debelle FD, Arlt VM *et al.* Early proximal tubule injury in experimental aristolochic acid nephropathy: functional and

- histological studies. *Nephrol. Dial. Transplant.* 2005; **20**: 2321–2332.
19. Pozdzik AA, Salmon IJ, Husson CP et al. Patterns of interstitial inflammation during the evolution of renal injury in experimental aristolochic acid nephropathy. *Nephrol. Dial. Transplant.* 2008; **23**: 2480–2491.
 20. Nagy J, Trinn C, Deak G, Schmelzer M, Burger T. The role of the tubulointerstitial changes in the prognosis of IgA glomerulonephritis. *Klin. Wochenschr.* 1984; **62**: 1094–1096.
 21. Tanaka A, Nishida R, Yokoi H, Kuwahara T. The characteristic pattern of aminoaciduria in patients with aristolochic acid-induced Fanconi syndrome: could aminoaciduria be the hallmark of this syndrome? *Clin. Nephrol.* 2000; **54**: 198–202.
 22. Tanaka A, Nishida R, Maeda K, Sugawara A, Kuwahara T. Chinese herb nephropathy in Japan presents adult-onset Fanconi syndrome: could different components of aristolochic acids cause a different type of Chinese herb nephropathy? *Clin. Nephrol.* 2000; **53**: 301–306.
 23. Tanaka A, Nishida R, Yoshida T, Koshikawa M, Goto M, Kuwahara T. Outbreak of Chinese herb nephropathy in Japan: are there any differences from Belgium? *Intern. Med.* 2001; **40**: 296–300.
 24. Yang SS, Chu P, Lin YF, Chen A, Lin SH. Aristolochic acid-induced Fanconi's syndrome and nephropathy presenting as hypokalemic paralysis. *Am. J. Kidney Dis.* 2002; **39**: E14.
 25. Lee S, Lee T, Lee B et al. Fanconi's syndrome and subsequent progressive renal failure caused by a Chinese herb containing aristolochic acid. *Nephrology (Carlton)* 2004; **9**: 126–129.
 26. Hong YT, Fu LS, Chung LH, Hung SC, Huang YT, Chi CS. Fanconi's syndrome, interstitial fibrosis and renal failure by aristolochic acid in Chinese herbs. *Pediatr. Nephrol.* 2006; **21**: 577–579.
 27. Jackson L, Kofman S, Weiss A, Brodovsky H. Aristolochic acid (NSC-50413): Phase I clinical study. *Cancer Chemother. Rep.* 1964; **42**: 35–37.
 28. Cronin AJ, Maidment G, Cook T et al. Aristolochic acid as a causative factor in a case of Chinese herbal nephropathy. *Nephrol. Dial. Transplant.* 2002; **17**: 524–525.
 29. Gillerot G, Jadoul M, Arlt VM et al. Aristolochic acid nephropathy in a Chinese patient: time to abandon the term "Chinese herbs nephropathy"? *Am. J. Kidney Dis.* 2001; **38**: E26.
 30. Hoshino J, Ubara Y, Tagami T et al. Chinese herbs and bone disease. *Intern. Med.* 2003; **42**: 345–350.
 31. Kanaan N, Cosyns JP, Jadoul M, Goffin E. The importance of a histology-based diagnosis of interstitial nephropathy in two patients with renal insufficiency. *Nephrol. Dial. Transplant.* 2003; **18**: 440–442.
 32. Lo SH, Wong KS, Arlt VM et al. Detection of Herba Aristolochia Mollisemae in a patient with unexplained nephropathy. *Am. J. Kidney Dis.* 2005; **45**: 407–410.
 33. Lord GM, Tagore R, Cook T, Gower P, Pusey CD. Nephropathy caused by Chinese herbs in the UK. *Lancet* 1999; **354**: 481–482.
 34. Nortier JL, Schmeiser HH, Muniz Martinez MC et al. Invasive urothelial carcinoma after exposure to Chinese herbal medicine containing aristolochic acid may occur without severe renal failure. *Nephrol. Dial. Transplant.* 2003; **18**: 426–428.
 35. Ubara Y, Katori H, Tagami T et al. Transcatheter renal arterial embolization therapy on a patient with polycystic kidney disease on hemodialysis. *Am. J. Kidney Dis.* 1999; **34**: 926–931.
 36. Yang L, Li X, Wang H. Possible mechanisms explaining the tendency towards interstitial fibrosis in aristolochic acid-induced acute tubular necrosis. *Nephrol. Dial. Transplant.* 2007; **22**: 445–456.
 37. Lo SH, Mo KL, Wong KS et al. Aristolochic acid nephropathy complicating a patient with focal segmental glomerulosclerosis. *Nephrol. Dial. Transplant.* 2004; **19**: 1913–1915.
 38. Meyer MM, Chen TP, Bennett WM. Chinese herb nephropathy. *Proc. (Bayl. Univ. Med. Cent.)* 2000; **13**: 334–337.
 39. Nishimagi E, Kawaguchi Y, Terai C, Kajiyama H, Hara M, Kamatani N. Progressive interstitial renal fibrosis due to Chinese herbs in a patient with calcinosis Raynaud esophageal sclerodactyly telangiectasia (CREST) syndrome. *Intern. Med.* 2001; **40**: 1059–1063.
 40. Vanherweghem JL, Tielemans C, Simon J, Depierreux M. Chinese herbs nephropathy and renal pelvic carcinoma. *Nephrol. Dial. Transplant.* 1995; **10**: 270–273.
 41. Yang HY, Lin JL, Chen KH, Yu CC, Hsu PY, Lin CL. Aristolochic acid-related nephropathy associated with the popular Chinese herb Xi Xin. *J. Nephrol.* 2006; **19**: 111–114.
 42. Martinez MC, Nortier J, Vereerstraeten P, Vanherweghem JL. Progression rate of Chinese herb nephropathy: impact of *Aristolochia fangchi* ingested dose. *Nephrol. Dial. Transplant.* 2002; **17**: 408–412.
 43. Kluth DC, Erwig LP, Rees AJ. Multiple facets of macrophages in renal injury. *Kidney Int.* 2004; **66**: 542–557.
 44. Rees AJ. The role of infiltrating leukocytes in progressive renal disease: implications for therapy. *Nat. Clin. Pract. Nephrol.* 2006; **2**: 348–349.
 45. Wilson HM, Walbaum D, Rees AJ. Macrophages and the kidney. *Curr. Opin. Nephrol. Hypertens.* 2004; **13**: 285–290.
 46. Zheng G, Wang Y, Mahajan D et al. The role of tubulointerstitial inflammation. *Kidney Int. Suppl.* 2005; **94**: S96–S100.
 47. Kim JY, Lim SW, Li C et al. Effect of FTY720 on chronic cyclosporine nephropathy in rats. *Transplantation* 2005; **80**: 1323–1330.
 48. Liu M, Chien CC, Burne-Taney M et al. A pathophysiologic role for T lymphocytes in murine acute cisplatin nephrotoxicity. *J. Am. Soc. Nephrol.* 2006; **17**: 765–774.
 49. Rabb H. The T cell as a bridge between innate and adaptive immune systems: implications for the kidney. *Kidney Int.* 2002; **61**: 1935–1946.
 50. Rodriguez-Iturbe B, Pons H, Herrera-Acosta J, Johnson RJ. Role of immunocompetent cells in nonimmune renal diseases. *Kidney Int.* 2001; **59**: 1626–1640.
 51. Wang Y, Wang YP, Tay YC, Harris DC. Progressive adriamycin nephropathy in mice: sequence of histologic and immunohistochemical events. *Kidney Int.* 2000; **58**: 1797–1804.
 52. Wang Y, Wang Y, Feng X et al. Depletion of CD4(+) T cells aggravates glomerular and interstitial injury in murine adriamycin nephropathy. *Kidney Int.* 2001; **59**: 975–984.
 53. Wang Y, Wang YP, Tay YC, Harris DC. Role of CD8(+) cells in the progression of murine adriamycin nephropathy. *Kidney Int.* 2001; **59**: 941–949.
 54. Vanherweghem JL, Abramowicz D, Tielemans C, Depierreux M. Effects of steroids on the progression of renal failure in chronic interstitial renal fibrosis: a pilot study in Chinese herbs nephropathy. *Am. J. Kidney Dis.* 1996; **27**: 209–215.
 55. Martinez MC, Nortier J, Vereerstraeten P, Vanherweghem JL. Steroid therapy in chronic interstitial renal fibrosis: the case of Chinese-herb nephropathy. *Nephrol. Dial. Transplant.* 2002; **17**: 2033–2034.
 56. Yoshimura E, Fujii M, Koide S et al. [A case of Chinese herbs nephropathy in which the progression of renal dysfunction was

- slowed by steroid therapy]. *Nippon Jinzo Gakkai Shi* 2000; **42**; 66–72.
57. Elenkov IJ. Glucocorticoids and the Th1/Th2 balance. *Ann. NY Acad. Sci.* 2004; **1024**; 138–146.
 58. Nortier JL, Schodt-Lanckman MM, Simon S *et al.* Proximal tubular injury in Chinese herbs nephropathy: monitoring by neutral endopeptidase enzymuria. *Kidney Int.* 1997; **51**; 288–293.
 59. Lebeau C, Arlt VM, Schmeiser HH *et al.* Aristolochic acid impedes endocytosis and induces DNA adducts in proximal tubule cells. *Kidney Int.* 2001; **60**; 1332–1342.
 60. Kabanda A, Jadoul M, Lauwerys R, Bernard A, Van Ypersele de Strihou C. Low molecular weight proteinuria in Chinese herbs nephropathy. *Kidney Int.* 1995; **48**; 1571–1576.
 61. Simoes ML, Hockley SL, Schwerdtle T *et al.* Gene expression profiles modulated by the human carcinogen aristolochic acid I in human cancer cells and their dependence on TP53. *Toxicol. Appl. Pharmacol.* 2008; **232**; 86–98.
 62. Gobe GC, Endre ZH. Cell death in toxic nephropathies. *Semin. Nephrol.* 2003; **23**; 416–424.
 63. Barker RN, Erwig LP, Hill KS, Devine A, Pearce WP, Rees AJ. Antigen presentation by macrophages is enhanced by the uptake of necrotic, but not apoptotic, cells. *Clin. Exp. Immunol.* 2002; **127**; 220–225.
 64. Strutz F, Neilson EG. New insights into mechanisms of fibrosis in immune renal injury. *Springer Semin. Immunopathol.* 2003; **24**; 459–476.
 65. Segerer S, Nelson PJ. Chemokines in renal diseases. *Sci. World J.* 2005; **5**; 835–844.
 66. Anders HJ, Vielhauer V, Schlondorff D. Chemokines and chemokine receptors are involved in the resolution or progression of renal disease. *Kidney Int.* 2003; **63**; 401–415.
 67. Leask A, Abraham DJ. TGF-beta signaling and the fibrotic response. *FASEB J.* 2004; **18**; 816–827.
 68. Bottinger EP. TGF-beta in renal injury and disease. *Semin. Nephrol.* 2007; **27**; 309–320.
 69. Tamaki K, Okuda S. Role of TGF-beta in the progression of renal fibrosis. *Contrib. Nephrol.* 2003; **139**; 44–65.
 70. Grandaliano G, Gesualdo L, Ranieri E *et al.* Monocyte chemotactic peptide-1 expression in acute and chronic human nephritides: a pathogenetic role in interstitial monocytes recruitment. *J. Am. Soc. Nephrol.* 1996; **7**; 906–913.
 71. Viedt C, Dechend R, Fei J, Hansch GM, Kreuzer J, Orth SR. MCP-1 induces inflammatory activation of human tubular epithelial cells: involvement of the transcription factors, nuclear factor-kappaB and activating protein-1. *J. Am. Soc. Nephrol.* 2002; **13**; 1534–1547.
 72. Kitamura A, Kitamura M, Nagasawa R *et al.* Renal fibroblasts are sensitive to growth-repressing and matrix-reducing factors from activated lymphocytes. *Clin. Exp. Immunol.* 1993; **91**; 516–520.
 73. Liu Y. Renal fibrosis: new insights into the pathogenesis and therapeutics. *Kidney Int.* 2006; **69**; 213–217.
 74. Schlondorff D. The role of chemokines in the initiation and progression of renal disease. *Kidney Int. Suppl.* 1995; **49**; S44–S47.
 75. Wang W, Koka V, Lan HY. Transforming growth factor-beta and Smad signalling in kidney diseases. *Nephrology (Carlton)* 2005; **10**; 48–56.
 76. Wynn TA. Cellular and molecular mechanisms of fibrosis. *J. Pathol.* 2008; **214**; 199–210.